

Concentration-dependent dye aggregation and disassembly triggered by the same artificial helical foldamer



Yuan Qiu^a, Haisi Hu^a, Dongxu Zhao^a, Jing Wang^a, Hong Wang^a, Qin Wang^a, Haiyan Peng^{a,b}, Yonggui Liao^{a,b,*}, Xiaolin Xie^{a,b}

^a Key Laboratory of Material Chemistry for Energy Conversion and Storage, Ministry of Education, Hubei Key Laboratory of Materials Chemistry and Service Failure, School of Chemistry and Chemical Engineering, Huazhong University of Science and Technology, Wuhan, 430074, China

^b National Anti-counterfeit Engineering Research Center, Huazhong University of Science and Technology, Wuhan, 430074, China

HIGHLIGHTS

- A novel strategy to achieve chiral H-aggregation and disassembly of cyanine dyes via changing [foldamer]/[dye] ratio.
- The new foldamer contains multiple binding sites, i.e., negatively charged pendants, helical grooves and cavities, for dyes.
- During the aggregation and disassembly, the solution color changes from peachblow to navy blue.

ARTICLE INFO

Keywords:
Artificial helical foldamer
Cyanine dye
H-aggregate

ABSTRACT

Constructing and regulating the cyanine dye aggregates have been constantly pursued because of their wide applications in photosensitizers, biological fluorescence probes, nonlinear optics, etc. However, to realize such a process using a single additive still remains a formidable challenge. Here, the aggregation and disassembly of positively charged 3,3-diethylloxadicyanin iodide (**DiOC₂(5)**) have been demonstrated just by changing the concentration of an artificial poly(phenylenediethynylene)-based helical foldamer (**Poly-1**) bearing L-alanine sodium pendants with an amide linker. **Poly-1** possessed the negatively charged pendants and hydrophobic helical grooves. Upon simple mixing of equal **DiOC₂(5)** and **Poly-1**, **DiOC₂(5)** molecules were mainly enriched on **Poly-1** surface driven by electrostatic interaction and arranged along the main chain of **Poly-1**, resulting in the formation of chiral H-aggregates. But, the excessive **Poly-1** would attract some **DiOC₂(5)** molecules in H-aggregates via electrostatic interaction. The isolated monomers were easy to orderly disperse into the helical grooves due to hydrophobic interaction. Meanwhile, during the aggregation and disassembly, the solution color changed from peachblow to purple red and then to purple and finally to navy blue.

1. Introduction

Cyanine dyes are a class of organic ionic compounds containing two heterocyclic components connected by a polymethine bridge with an odd number of conjugated carbon atoms [1]. Their aggregates have attracted considerable attention for their wide applications including photosensitizers [2], biological fluorescence probes [3] and nonlinear optics [4]. To realize these applications, the construction and regulation of the cyanine dye aggregates are of great importance. Due to the ionic nature as well as π - π stacking and van der Waals forces, cyanine dyes can self-aggregate in aqueous solution by changing the concentration, ionic strength, pH or temperature [5]. Besides, liposomes [6],

biopolymers [7,8] and some artificial polymers [9,10] have been used as the additives to construct the assembled cyanine dye aggregates. In many cases, J- or H-aggregates can be obtained when the dyes stack in a head-to-tail or face-to-face way, respectively [11]. In spite of many methods to construct J- or H-aggregates, rare attempts to further regulate the aggregates have been reported. For example, enhanced J-aggregation of a cyanine dye has been achieved in the presence of a large excess carboxymethyl amylose, leading to a super-helical complex of cyanine dye/carboxymethyl amylose [12]. J-aggregates for pseudoisocyanine or H-aggregates for pinacyanol are decreased by the moderate binding of cucurbit[7]uril with pseudoisocyanine or pinacyanol [13]. A cycling switch among four kinds of aggregates for a cyanine dye have

* Corresponding author. Key Laboratory of Material Chemistry for Energy Conversion and Storage, Ministry of Education, Hubei Key Laboratory of Materials Chemistry and Service Failure, School of Chemistry and Chemical Engineering, Huazhong University of Science and Technology, Wuhan, 430074, China.

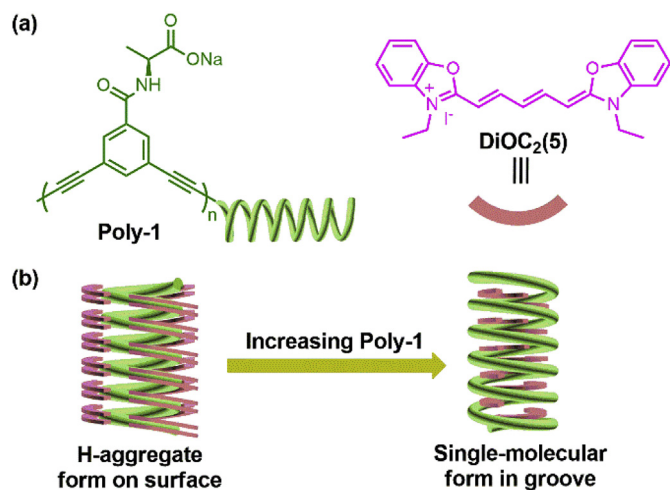
E-mail address: ygliao@mail.hust.edu.cn (Y. Liao).

<https://doi.org/10.1016/j.polymer.2019.02.063>

Received 29 January 2019; Received in revised form 26 February 2019; Accepted 28 February 2019

Available online 05 March 2019

0032-3861/ © 2019 Elsevier Ltd. All rights reserved.



Scheme 1. Illustrative process of concentration-dependent $\text{DiOC}_2(5)$ aggregation and disassembly.

been achieved by adding Tb^{3+} and then EDTA [5]. Obviously, the addition of extra additives can further regulate the aggregates.

In recent years, artificial foldamers have garnered a lot of interest because they can mimic the folding behavior that occurs in the secondary structure of biopolymer [14]. Thus, these three-dimensional foldamers possess a characteristic asymmetric groove and cavity [15]. When guest molecules are bound to the foldamers, they can insert into the groove or cavity [16,17]. In this regard, the foldamers can provide multiple binding sites and thus emerge as new additives to regulate cyanine dye aggregates. On the other hand, the foldamers can also be used to construct the aggregates at the same time when the charged pendants are conjugated to the main chain. The electrostatic interactions between the charged pendants and dyes may promote the dye aggregation. For this purpose, we have designed a poly(phenylene-diethynylene)-based foldamer (**Poly-1**) bearing L-alanine sodium pendants with an amide linker as a novel additive for constructing and regulating the cyanine dye aggregates (Scheme 1a). The helical folding behavior of **Poly-1** in water was driven by the hydrophobic interaction. This helical structure was further stabilized via π - π stacking between phenylenediethynylene units and electrostatic repulsion between the adjacent negatively charged pendants. In addition, **Poly-1** helix features π - π stacked aromatic residues similar to the π - π stacked bases in DNA and the negatively charged pendants like the phosphate groups on DNA. Herein, we use **Poly-1** to complex with the cyanine dye, 3,3-diethyloxadicarbocyanine iodide ($\text{DiOC}_2(5)$, Scheme 1a), in aqueous solution. The system demonstrates that the concentration-dependent aggregation and disassembly of the dye have been achieved. Meanwhile, the color changes during the process can be directly observed by naked eye.

2. Experimental section

2.1. Materials

L-Alanine and thionyl chloride were purchased from Sahn Chemical Technology Co., Ltd. 4-(4,6-Dimethoxy-1,3,5-triazin-2-yl)-4-methylmorpholinium chloride (DMT-MM) was purchased from J&K Chemical Co., Ltd. Copper(I) chloride, *N,N,N',N'*-tetramethylethylenediamine (TMEDA) and ultrapure water were purchased from Alfa Aesar. Triethylamine (TEA) was dried over potassium hydroxide and distilled under nitrogen. Tetrahydrofuran (THF) was dried over sodium benzophenone ketyl and distilled onto LiAlH_4 . *N,N*-dimethylformamide (DMF) was distilled from calcium hydride. 3,5-Diethynyl-benzoic acid was prepared according to a previous literature [15].

2.2. Characterization

^1H and ^{13}C NMR spectra were recorded using a Bruker AVANCE III-400 instrument at room temperature. FTIR spectra were obtained with a Bruker Equinox 55 spectrometer. The number-average molecular weight (M_n) and the polydispersity (M_w/M_n) were determined on a size exclusion chromatography (SEC) apparatus equipped with a JASCO PU-980 Intelligent pump and a JASCO RI-930 Intelligent RI detector. DMF containing lithium chloride (0.01 M) was used as the eluent at a flow rate of 0.4 mL min^{-1} at 40°C . The molecular weight calibration curve was obtained with polystyrene standard. The solution pH was measured with an AS-600 pH meter. The electron spray ionization mass spectra (ESI-MS) were measured on a Bruker micrOTOF-Q II spectrometer. The specific optical rotation values ($[\alpha]_{20}^D$) were obtained from a WZZ-2B polarimeter (Shanghai ShenGuang Instrument Co., Ltd.). The circular dichroism (CD) spectra were recorded on a JASCO J-810 spectropolarimeter. The ultraviolet–visible (UV–vis) absorption spectra were recorded on a PerkinElmer Lambda 35 spectrophotometer. The fluorescence spectra were measured on a JASCO FP-6500 spectrofluorescence. Isothermal titration calorimetry (ITC) measurements were carried out at $25.00 \pm 0.01^\circ\text{C}$ on a MicroCal iTC200 apparatus. Atomic force microscope (AFM) images were acquired in tapping mode with a Shimadzu SPM-9700 instrument, performed at ambient temperature in air using standard silicon cantilevers with a spring constant of about 40 N/m , a tip radius of 5–10 nm, and a resonance frequency of $\sim 300 \text{ kHz}$.

2.3. Synthesis of compound 2

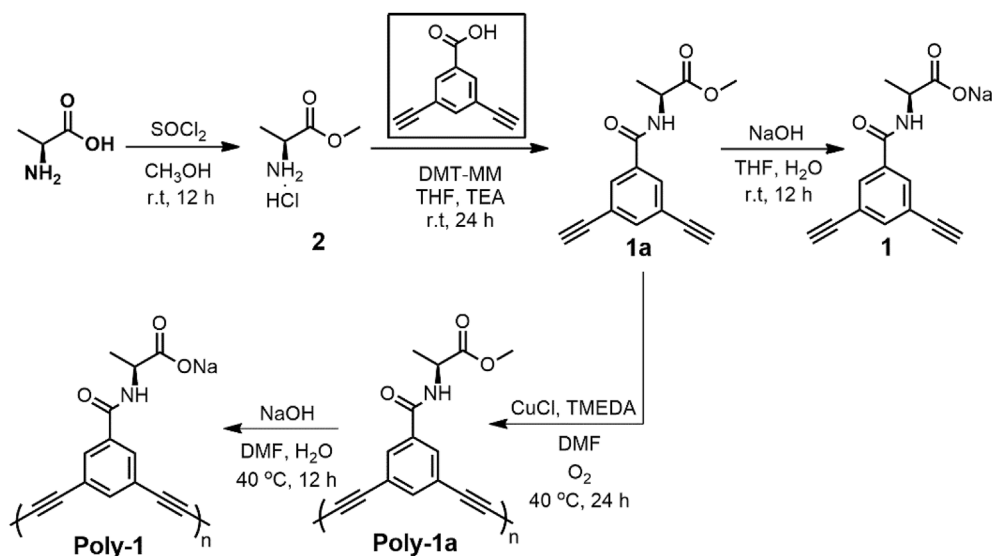
Thionyl chloride (12.2 mL, 168.5 mmol) was added to methanol (66 mL) at 0°C , and the resulting solution was stirred for 10 min. L-Alanine (3.0 g, 33.7 mmol) was then added to the solution, and the resulting mixture was stirred at room temperature overnight. The solvent was evaporated and dried in vacuum to obtain 2 as colorless oil (4.56 g, 97%). $[\alpha]_{20}^D = +6.8^\circ$ ($c = 2 \text{ g/dL}$, in methanol). ^1H NMR (400 MHz, $\text{DMSO-}d_6$, TMS, ppm): $\delta = 8.71$ (s, $-\text{NH}_3\text{Cl}$, 3H), 4.05 (q, $J = 7.2 \text{ Hz}$, $-\text{CH-CH}_3$, 1H), 3.74 (s, $-\text{O-CH}_3$, 3H), 1.43 (d, $J = 7.2 \text{ Hz}$, $-\text{CH-CH}_3$, 3H).

2.4. Synthesis of compound 1a

To a mixture of 3,5-diethynyl-benzoic acid (1.0 g, 5.80 mmol) and 2 (1.05 g, 7.54 mmol) in anhydrous THF (29 mL) were added 4-(4,6-dimethoxy-1,3,5-triazin-2-yl)-4-methylmorpholinium chloride (DMT-MM) (3.21 g, 11.6 mmol) and dry TEA (4.2 mL, 30.2 mmol). The mixture was stirred at room temperature for 24 h and the solvent was concentrated under reduced pressure. The residue was dissolved in ethyl acetate, and washed with 0.5 M HCl, saturated solution of sodium bicarbonate, and brine and dried over anhydrous sodium sulfate. After filtration, the solvent was removed by evaporation, and the residue was then purified by column chromatography (SiO_2 , petroleum ether/ethyl acetate = 5/1, v/v) to afford 1a as a white solid (1.08 g, 72%). $[\alpha]_{20}^D = +5.9^\circ$ ($c = 2 \text{ g/dL}$, in DMF). ^1H NMR (400 MHz, $\text{DMSO-}d_6$, TMS, ppm): $\delta = 9.01$ (d, $J = 6.8 \text{ Hz}$, $-\text{NH-}$, 1H), 8.01 (s, Ar-H, 2H), 7.75 (s, Ar-H, 1H), 4.52–4.45 (m, $-\text{NH-CH-}$, 1H), 4.40 (s, $-\text{C}\equiv\text{CH}$, 2H), 3.65 (s, $-\text{O-CH}_3$, 3H), 1.41 (d, $J = 7.6 \text{ Hz}$, $-\text{CH-CH}_3$, 3H). ^{13}C NMR (100 MHz, $\text{DMSO-}d_6$, TMS, ppm): $\delta = 173.4$ ($-\text{CO-}$ (ester)), 164.8 ($-\text{CO-}$ (amide)), 137.4 (aromatic), 135.0 (aromatic), 131.4 (aromatic), 123.1 (aromatic), 82.9 ($-\text{C}\equiv\text{CH}$), 82.2 ($-\text{C}\equiv\text{CH}$), 52.4 ($-\text{O-CH}_3$), 48.9 ($-\text{CH-NH-}$), 17.1 ($-\text{CH-CH}_3$). IR (KBr, cm^{-1}): 3311 ($\equiv\text{C-H}$), 3285 (N-H), 2106 ($\text{C}\equiv\text{C}$), 1729 (C=O), 1634 (C=O). HRMS (ESI-MS): m/z calcd for $[\text{M}(\text{C}_{15}\text{H}_{13}\text{NO}_3) + \text{Na}]^+$, 278.0895; found 278.0882.

2.5. Synthesis of compound 1

To a solution of 1a (0.3 g, 1.18 mmol) in THF (5 mL) was added a

Scheme 2. Synthetic route for foldamer **Poly-1**.

solution of sodium hydroxide (0.05 g, 1.18 mmol) in water (5 mL). The mixture was stirred at room temperature overnight and the solvent was concentrated under reduced pressure. The residue was dissolved in water, and washed with chloroform three times. The water was removed by evaporation, and the residue was purified by recrystallization from water/methanol (8/2, v/v) to afford **1** as a white crystalline solid (0.19 g, 60%). $[\alpha]_{20}^D = +27.5^\circ$ ($c = 2$ g/dL, in water). $^1\text{H NMR}$ (400 MHz, DMSO- d_6 , TMS, ppm): $\delta = 8.23$ (d, $J = 6.4$ Hz, $-\text{NH}-$, 1H), 7.90 (s, Ar- H , 2H), 7.69 (s, Ar- H , 1H), 4.38 (s, $-\text{C}\equiv\text{CH}$, 2H), 4.03–3.96 (m, $-\text{NH}-\text{CH}_2-$, 1H), 1.28 (d, $J = 6.8$ Hz, $-\text{CH}-\text{CH}_3$, 3H). $^{13}\text{C NMR}$ (100 MHz, DMSO- d_6 , TMS, ppm): $\delta = 175.8$ ($-\text{CO}-$ (carboxylate)), 163.5 ($-\text{CO}-$ (amide)), 137.0 (aromatic), 136.6 (aromatic), 131.0 (aromatic), 122.9 (aromatic), 82.7 ($-\text{C}\equiv\text{CH}$), 82.3 ($-\text{C}\equiv\text{CH}$), 51.0 ($-\text{CH}-\text{NH}-$), 19.4 ($-\text{CH}-\text{CH}_3$). IR (KBr, cm^{-1}): 3321 ($\equiv\text{C}-\text{H}$), 3289 (N-H), 2105 ($\text{C}\equiv\text{C}$), 1627 ($\text{C}=\text{O}$), 1583 ($\text{C}=\text{O}$). HRMS (ESI-MS): m/z calcd for $[\text{M}(\text{C}_{14}\text{H}_{10}\text{NO}_3\text{Na}) + \text{Na}]^+$, 286.0456; found 286.0446.

2.6. Polymerization of **1a**

1a (0.8 g, 3.11 mmol), N,N,N',N' -tetramethylethylenediamine (TMEDA) (1.08 g, 9.32 mmol), and CuCl (0.09 g, 0.932 mmol) were dissolved in DMF (31 mL). The mixture was stirred at 40 °C with oxygen bubbling. After 24 h, the solution was precipitated into a large amount of acetone acidified with 37 wt % HCl solution. The precipitate was collected by centrifugation, washed with acetone, and then dried in vacuum to afford **Poly-1a** as a pale yellow solid (0.64 g, 80%). $M_n = 2.07 \times 10^4$, $M_w/M_n = 2.89$. $^1\text{H NMR}$ (400 MHz, DMSO- d_6 , TMS, ppm): $\delta = 9.03$ – 7.84 (m, Ar- H , 3H), 4.46 (brs, $-\text{NH}-\text{CH}_2-$, 1H), 3.66 (brs, $-\text{O}-\text{CH}_3$, 3H), 1.42 (brs, $-\text{CH}-\text{CH}_3$, 3H). IR (KBr, cm^{-1}): 3301 (N-H), 2212 ($\text{C}\equiv\text{C}$), 1732 ($\text{C}=\text{O}$), 1640 ($\text{C}=\text{O}$).

2.7. Hydrolysis of **Poly-1a**

To a solution of **Poly-1a** (0.64 g) in DMF (24.9 mL) was added a solution of sodium hydroxide (0.60 g, 14.9 mmol) in water (24.9 mL). The reaction mixture was stirred at room temperature overnight and dialyzed against ultrapure water with 3.5 kDa. After 72 h, the solvent was concentrated by evaporation, and the residue was precipitated into a large amount of acetone. The resultant precipitate was collected by centrifugation, washed with acetone, and dried under vacuum to afford **Poly-1** as a brown solid (0.57 g, 89%). $^1\text{H NMR}$ (400 MHz, DMSO- d_6 , TMS, ppm): $\delta = 9.07$ – 7.69 (m, Ar- H , 3H), 4.40 (brs, $-\text{NH}-\text{CH}_2-$, 1H), 1.42 (brs, $-\text{CH}-\text{CH}_3$, 3H). IR (KBr, cm^{-1}): 3301 (N-H), 2213 ($\text{C}\equiv\text{C}$), 1633

($\text{C}=\text{O}$), 1579 ($\text{C}=\text{O}$).

2.8. Sample preparation for CD, UV-vis absorption and fluorescence measurements

Ultrapure water was degassed with nitrogen and a borate buffer (pH 7.8) was made for these measurements. The concentration of monomer unit was chosen as the concentration of **Poly-1**.

2.9. Isothermal titration calorimetry (ITC) measurements

In a typical run, 200 μL of 0.1 mM aqueous solution of **DiOC₂(5)** was placed in the sample cell and then titrated dropwise with 2 μL of 1 mM **Poly-1** in water. The titrations consist of the first 0.4 μL injection and followed 19 injection of 2 μL with 20 s duration at 150 s equilibration time interval. The titration of **Poly-1** in syringe into water in the sample cell without **DiOC₂(5)** was used as a control to obtain the dilution heat. All solutions were degassed prior to titration. A binding isotherm curve was obtained by plotting the total heat per injection (kJ mol^{-1} of injectant) as a function of the molar ratio ($[\text{Poly-1}]/[\text{DiOC}_2(5)]$). All the data were analyzed with Microcal Origin 7.0 software.

3. Results and discussion

3.1. Synthesis of foldamer **Poly-1**

The foldamer was synthesized via the route illustrated in Scheme 2. At first, the condensation of 3,5-diethynylbenzoic acid with compound **2** proceeded using 4-(4,6-dimethoxy-1,3,5-triazin-2-yl)-4-methylmorpholinium chloride (DMT-MM) as a catalyst to afford the novel monomer **1a**. Then, **1a** was polymerized through Glaser-Hay coupling reaction with CuCl and N,N,N',N' -tetramethylethylenediamine (TMEDA) in DMF under an oxygen atmosphere. The disappearance of the acetylene protons of **1a** at 4.38 ppm demonstrated the successful polymerization (Figs. S1 and S5). The resultant **Poly-1a** was soluble in DMF and DMSO, while insoluble in dichloromethane, chloroform, THF, methanol and water. The number-average molecular weight (M_n) and polydispersity (M_w/M_n) were estimated to be 2.07×10^4 and 2.89 (Fig. S7), respectively. Finally, the hydrolysis of **Poly-1a** afforded the amphiphilic **Poly-1** containing the hydrophobic phenylenediethynylene backbone and a hydrophilic side chain. $^1\text{H NMR}$ analysis failed to confirm the completion of the reaction because the signal of the methyl

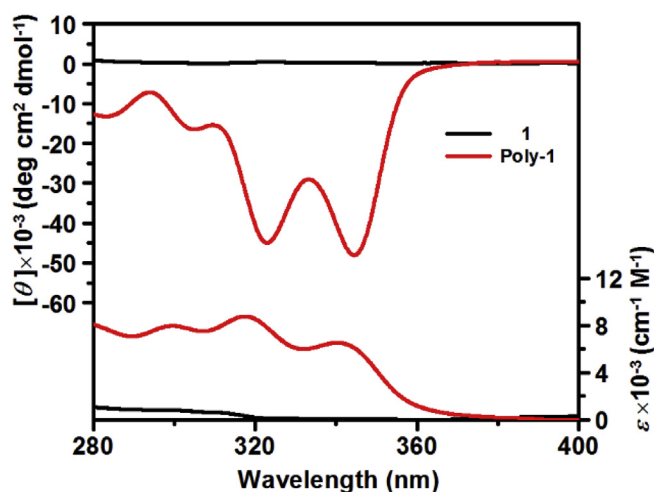


Fig. 1. CD (up) and UV-vis absorption (bottom) spectra of **1** and **Poly-1** in water. All spectra were measured in a 1 mm quartz cell at ambient temperature. $[1] = [\text{Poly-1}] = 0.62 \text{ mM}$.

ester moiety at 3.66 ppm would be shielded by water peak (Fig. S6). Fortunately, FTIR spectra demonstrated the hydrolysis by the absence of absorption band at 1732 cm^{-1} for C=O stretching due to methyl ester and presence of absorption band at 1579 cm^{-1} for C=O stretching due to carboxylate sodium (Fig. S8) [18]. **Poly-1** was insoluble in dichloromethane, chloroform, THF and DMF, but partially soluble in DMSO and methanol, while quite in water. In particular, the number-average degree of polymerization (N) of **Poly-1** was considered to be the same as that of **Poly-1a** because the conditions for hydrolysis reaction were mild to the backbone structure.

3.2. Helical folding of **Poly-1**

The helical folding behavior of **Poly-1** was studied by CD and UV-vis absorption spectra. The concentration of monomer unit was chosen as the concentration of **Poly-1**. As shown in Fig. 1, monomer **1** exhibited weak absorption peak at 300 nm, which was ascribed to phenyl rings [19], and no absorption was observed above 318 nm. However, three absorption peaks were found at 300, 318 and 340 nm for **Poly-1**. The former absorption peak was again assigned to phenyl rings, while the latter two to the polymer main chain. In addition, monomer **1** showed no Cotton effects in water at wavelengths greater than 300 nm. But strong negative Cotton effects were observed at 323 and 344 nm. These results indicated that the observed Cotton effects for **Poly-1** were not attributed to the chiral center of **1** or intermolecular chiral assembly, but attributed to the helical chirality of the main chain [20]. In other words, **Poly-1** main chain definitely possessed a preferred-handed folded helix in water.

Next, we investigated helical folding mechanism of **Poly-1**. Due to the amphiphilic nature of **Poly-1**, the helical folding in water could be driven by hydrophobic effect [21]. Moreover, this behavior would occur in a preferred-handed screw sense directed by L-alaninate sodium pendants. Usually, the folded helical structures could be stabilized by intramolecular hydrogen bonding and/or the π - π stacking interaction [22]. The H/D exchange experiments based on solution-state FTIR spectra of monomer **1** and **Poly-1** were conducted in the dilute solution (20 mM) to determine the presence/absence of hydrogen bonding (Fig. 2). For monomer **1**, the absorption band at 1637 cm^{-1} corresponded to the C=O stretching amide I band. Interestingly, no amide II band of N-H bending was observed in D_2O at the range from 1570 to 1515 cm^{-1} , but the amide II' absorption band of N-D bending at 1446 cm^{-1} appeared due to the deuterated NH groups [23]. These results suggested that the amide groups in monomer **1** formed hydrogen bonds with water. Similar results could be found for **Poly-1** in D_2O . The

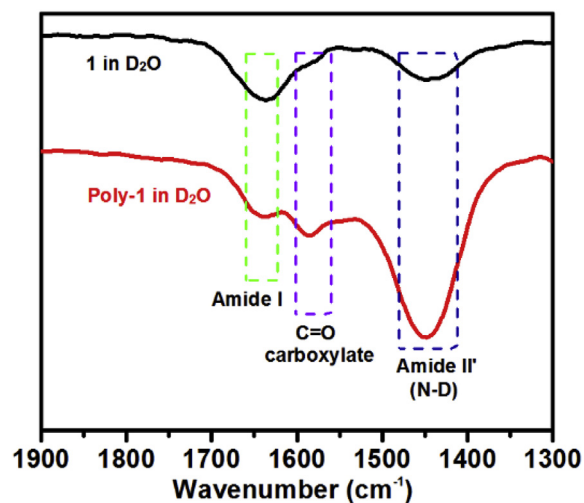


Fig. 2. FTIR spectra of **1** and **Poly-1** in D_2O at ambient temperature. $[1] = [\text{Poly-1}] = 20 \text{ mM}$.

spectrum of **Poly-1** showed amide I band at 1639 cm^{-1} and amide II' band at 1448 cm^{-1} instead of amide II band in D_2O , also implying that NH groups were accessible to water. Namely, hydrogen bonding was not a stabilizing force to the helical structure in **Poly-1**.

To confirm whether π - π stacking interaction between the phenylenediethynylene units was the stabilizing force to the helical structure in **Poly-1**, we investigated the fluorescence spectra of **Poly-1** in mixed DMSO/water. Compared to water, DMSO was a good solvent for the phenylenediethynylene backbone. As shown in Fig. 3a, the fluorescence intensity of **Poly-1** at around 570 nm significantly decreased with increasing water content. The low fluorescence intensity in water was a typical result of helical folding attributed to the strong π - π stacking interaction between phenylenediethynylene units of **Poly-1** [24,25]. Also, this result was further confirmed by the UV-vis absorption spectra. When the content of water increased, an apparent hypochromic effect was observed with a slight red shift from 338 to 340 nm in the main chain (Fig. 3b), which was described as the promotion of π - π stacking interaction [26]. Obviously, π - π stacking interaction was a stabilizing force to the helical structure in **Poly-1**.

Interestingly, the electrostatic repulsion existed between the adjacent negatively charged pendants in **Poly-1**. To determine its role in stabilizing the helical structure, we investigated the effect of different NaCl concentration on the degree of the preferred-handedness of **Poly-1** at $[\theta]_{\text{max}}$ wavelengths. In particular, the degree of the preferred-handedness was evaluated by the Kuhn dissymmetry factor $g (= \Delta\epsilon/\epsilon)$, in which $\Delta\epsilon = [\theta]/3298$ [27]. Fig. S9 showed that the g -value decreased by 12% with increasing NaCl concentration, indicating that the helix-forming ability of **Poly-1** was decreased [22]. The presence of NaCl was anticipated to shield the charged pendants so that the electrostatic repulsion was weakened. Meanwhile, the dehydration of NaCl attenuated the hydration of the pendants [28]. As a result, the polymer chain started to shrink, which was unfavorable for the helix formation. Therefore, these results demonstrated that the helical folding behavior of **Poly-1** in water was mainly driven by the hydrophobic effect and this helical structure was further stabilized via π - π stacking interaction and electrostatic repulsion.

Fig. 3c showed that the Cotton effects for **Poly-1** were varied at different DMSO/water ratios. The relatively weak Cotton effects were observed at DMSO/water of 9/1, indicating that **Poly-1** adopted a helical structure to some extent. However, the Cotton effect intensities increased by about 4-fold in the presence of 80 vol% of water. Further addition of water led to $\sim 14.2\%$ decrease. These results implied that the degree of the preferred-handedness for **Poly-1** could be modulated in the mixtures of DMSO and water. In contrast, the g -values of **Poly-1**

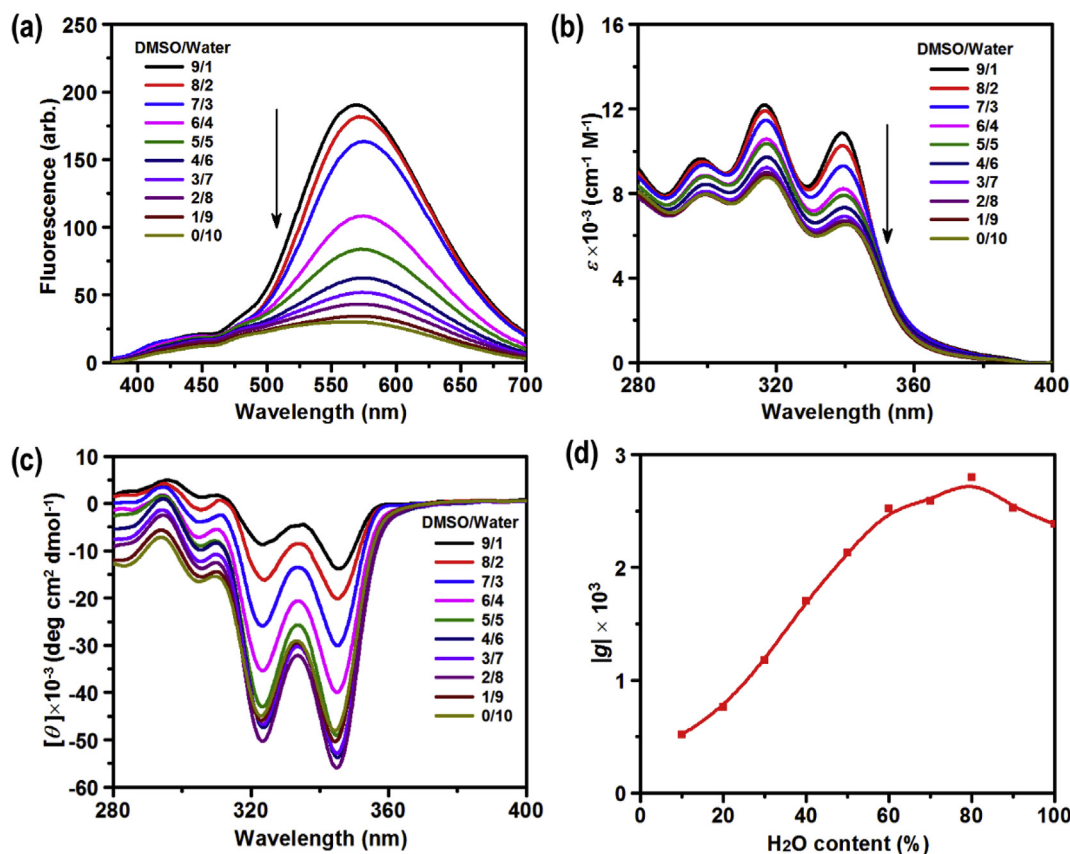


Fig. 3. Fluorescence (a; $\lambda_{\text{ex}} = 360$ nm), UV-vis absorption (b) and CD spectra (c) of **Poly-1** in DMSO/water (v/v). (d) Effect of water content on g -values of **Poly-1** at the $[\theta]_{\text{max}}$ wavelengths. All spectra were measured in a 1 mm quartz cell at ambient temperature. $[\text{Poly-1}] = 0.62$ mM.

at $[\theta]_{\text{max}}$ wavelengths were also calculated. As shown in Fig. 3d, the g -value reached a maximum at a DMSO/water ratio of 2/8, which indicated that the helix-forming ability of **Poly-1** was enhanced at this ratio [22]. However, **Poly-1** still showed a good helix-forming ability in water with a g value as high as 2.38×10^{-3} , only 14.7% less than the maximum value. In order to simplify the system, we chose water as solvent for the subsequent investigations.

3.3. Concentration-dependent **DiOC₂(5)** aggregation and disassembly

Fig. 4a showed that the aqueous solutions of the pure **Poly-1** and **DiOC₂(5)** were colorless and peachblow, respectively. Upon mixing **Poly-1** into **DiOC₂(5)** aqueous solution, various colors from peachblow to purple red and then to purple and finally to navy blue could be observed immediately when the concentration of **Poly-1** increased from 0 to 16 equiv (Fig. 4a). This result suggested that there existed some specific interactions between **Poly-1** and **DiOC₂(5)** and these interactions would be changed at different ratios.

UV-vis absorption spectra of the pure **Poly-1** and **DiOC₂(5)** with different content of **Poly-1** in water were measured (Fig. 4b and Fig. S10a). For **Poly-1**, no absorption peak was found in the wavelength range of 450–700 nm. The pure **DiOC₂(5)** featured the monomer absorption band at 576 nm with a vibrational shoulder at about 548 nm [29]. When the concentration of **Poly-1** increased from 0 to 0.6 equiv, the absorption at 576 nm gradually decreased and finally blue-shifted to 533 nm, indicative of the transformation of **DiOC₂(5)** monomers to face-to-face π -stacked dimers (H-dimers) [30]. In addition, an isosbestic point at 530 nm clearly suggested an equilibrium between monomer and dimer. As the concentration of **Poly-1** was increased to 1.0 equiv, the absorption curves did not pass the isosbestic point and the dimeric absorption band at 533 nm took a blue-shift to 527 nm. These results

implied a higher aggregate beyond the dimeric stage for **DiOC₂(5)** was obtained [31]. The solution color changed from peachblow to purple red. Plotting the absorption band at 527 nm versus the concentration of **Poly-1** revealed that the formation process of the aggregates was accomplished in the presence of 1.0 equiv of **Poly-1**, corresponding to a ratio of one monomer unit per **DiOC₂(5)** (Fig. S10b). However, the aggregates started to disassemble into dimer (540 nm) and monomer (598 nm) in the presence of 2.0 equiv of **Poly-1**, resulting in a light purple solution. Upon further addition of **Poly-1** to 4.0 equiv, the absorption band in the dimer was red-shifted to 552 nm, accompanied with a slight hyperchromic effect. At the same time, the absorption band at 598 nm also showed the hyperchromic effect. As a result, the light purple solution transformed to deep purple. Interestingly, the spectral shape seemingly returned to the original one by loading 16 equiv of **Poly-1**, in spite of about 22 nm red-shift from the original one. So, a navy blue solution was obtained. Figs. S10b and S10c showed, upon further increasing **Poly-1**, there were almost no consistent red-shift and hyperchromic effect of the resultant absorption band, clearly indicating that the disassembly process completed.

To determine the type of the aggregates, CD measurement was conducted. As shown in Fig. 5, the pure **DiOC₂(5)** displayed no CD signal. However, upon addition of **Poly-1** from 0 to 1.0 equiv, the positive CD signals at 520 nm for H-dimers and the negative at 476 nm were observed, which was centered at 505 nm. Such biphasic CD signals were attributed to the exciton coupling interaction between the adjacent H-dimers. This suggested that the dimers were arranged on the top of each other, resulting in formation of the higher aggregates, i.e. H-aggregates [32]. When an excess of **Poly-1** was added, the biphasic CD signals disappeared due to the absence of exciton coupling interaction among dimers [33]. Meanwhile, an increasing intensity of CD signal at 606 nm for the monomeric **DiOC₂(5)** and a decreasing at 520 nm could

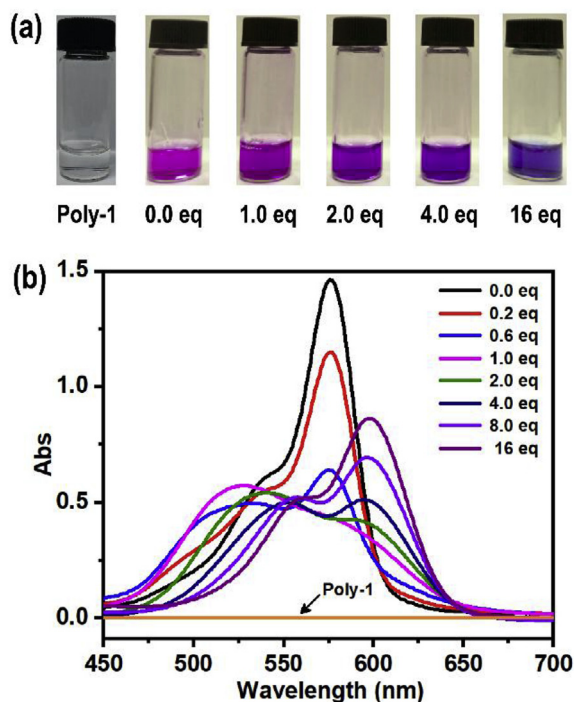


Fig. 4. (a) Sample colors corresponding to the pure Poly-1 and DiOC₂(5) with different content of Poly-1. (b) UV-vis absorption spectra of the pure Poly-1 and DiOC₂(5) in the presence of Poly-1 in water. All spectra were measured in a 2 mm quartz cell at ambient temperature. The concentrations of the pure Poly-1 and DiOC₂(5) were 832 and 52 μM, respectively. (For interpretation of the references to color in this figure legend, the reader is referred to the Web version of this article.)

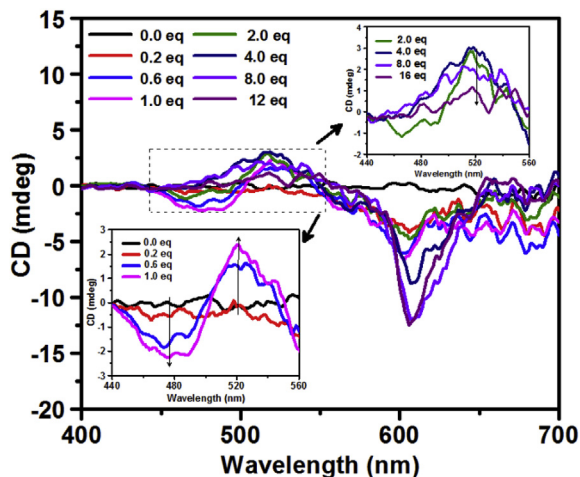


Fig. 5. CD spectra of DiOC₂(5) in the presence of Poly-1 in water. The inset showed the range from 440 to 560 nm. All spectra were measured in a 1 mm quartz cell at ambient temperature. [DiOC₂(5)] = 52 μM.

be seen. At last, only a single CD signal at 606 nm remained, indicative of the complete disassembly of H-aggregates to monomers.

Fluorescence spectra were also performed to further confirm the formation and disassembly of H-aggregates. As shown in Fig. S11a, the pure DiOC₂(5) showed a fluorescence at 611 nm in aqueous solution upon excited at 470 nm. However, the addition of Poly-1 gradually decreased the fluorescence intensity, which reached a minimum in the presence of 1.0 equiv of Poly-1 (Fig. S11b). This result also verified the formation of H-aggregates which usually acted as the poor emitters [34]. Further addition of Poly-1 resulted in a red-shift of fluorescence

signal from 611 to 644 nm along with a modest intensity enhancement. This was in good agreement with the disassembly of H-aggregates, because the isolated DiOC₂(5) molecules did not show aggregation-caused quenching (ACQ) behavior any more [35].

3.4. Binding mode of DiOC₂(5) to Poly-1

The above UV-vis absorption, CD and fluorescence spectral changes revealed that DiOC₂(5) could be bound to Poly-1. For insight understanding of the binding behavior, the binding modes of DiOC₂(5) to Poly-1 were explored. We initially performed the AFM measurements for Poly-1 in the absence and presence of DiOC₂(5). Samples for AFM measurements were prepared by spin coating dilute solutions onto freshly-cleaved mica substrates and then dried in vacuum overnight. As shown in Fig. 6a and b, Fig. S12a and S12b, the average heights of Poly-1 and DiOC₂(5) were approximately 1.66 ± 0.21 and 0.43 ± 0.04 nm, respectively. The swollen height for Poly-1 with fully conjugated backbone could be estimated using the radius of gyration of a worm-like chain [36,37], $R_g = (Nb^2/12)^{1/2}$, where the degree of polymerization $N = 82$ for Poly-1 and average statistical segment length $b = 0.68$ nm [38–41] were taken.

Moreover, the height of the dried polymer in vacuo was usually about 40% of the diameter ($2R_g$) of swollen one [42,43]. As a result, the estimated dried height was about 1.42 nm, which was in agreement with that obtained from AFM observation at ambient atmosphere. This result also implied that single chain of Poly-1 was well dispersed in such a dilute aqueous solution. The average height increased to 2.04 ± 0.25 nm after complexation with 1.0 equiv of DiOC₂(5), indicative of the mode of surface binding (Fig. 6c and Fig. S12c) [44]. In other words, DiOC₂(5) H-aggregates were arranged on the periphery of Poly-1 helix. In contrast, after the complete disassembly of H-aggregates, the complex featured an average height of 1.67 ± 0.23 nm which was similar to that of pure Poly-1 (Fig. 6d and Fig. S12d). Such a case excluded the possibility of surface binding.

Then, the ¹H NMR spectra measurements of DiOC₂(5) in absence and presence of Poly-1 (Fig. 7) were also conducted. The obvious resonance absorptions of aromatic protons assigned to DiOC₂(5) appeared ranging from 8 to 7 ppm in D₂O, but disappeared completely after the addition of 16 equiv of Poly-1. These results indicated that DiOC₂(5) was entrapped within Poly-1 helix, and thus the aromatic signals were shielded [30]. Interestingly, these signals appeared again when the system was treated with DMSO-*d*₆ (D₂O/DMSO-*d*₆ = 6/4), which still gave rise to a good helix-forming ability of Poly-1 (Fig. 3d). In other words, the shielding effect at this moment was weakened because DiOC₂(5) molecules were released from the well-defined Poly-1 helix. These results implied a fact that DiOC₂(5) was inserted into the helical groove or the cavity of Poly-1 helix in water.

However, we still needed to distinguish whether DiOC₂(5) was bound to Poly-1 via intercalation or groove binding. Fluorescence quenching experiments using negatively charged iodide ion as a quencher would clarify the binding mode. Fluorescence quenching could be analyzed using the Stern-Volmer equation, $F_0/F = 1 + K_{sv}[Q]$, where F_0 and F were fluorescence intensities in the absence and presence of the quencher Q . The dynamic quenching constant (K_{sv}) was calculated if plot of F_0/F against $[Q]$ displays a linear trend [45]. In general, intercalative binding of a fluorophore led to a reduction in fluorescence quenching because intercalation could protect the fluorophore, to which the approach of the quencher was restricted [46]. In contrast, for groove binding, the quenching efficiency should be improved in the addition of a quencher like KI. The phenomenon was associated with the change in ionic strength. The increase in the ionic strength resulted in the release of the fluorophore from the groove and thus a decrease in fluorescence yield [47]. As shown in Fig. 8, in aqueous solution KI quenched the fluorescence of DiOC₂(5) effectively and K_{sv} value of DiOC₂(5) was estimated to be 24.9 M^{-1} . More importantly, the Stern-Volmer plot obtained by addition of KI to the complex of

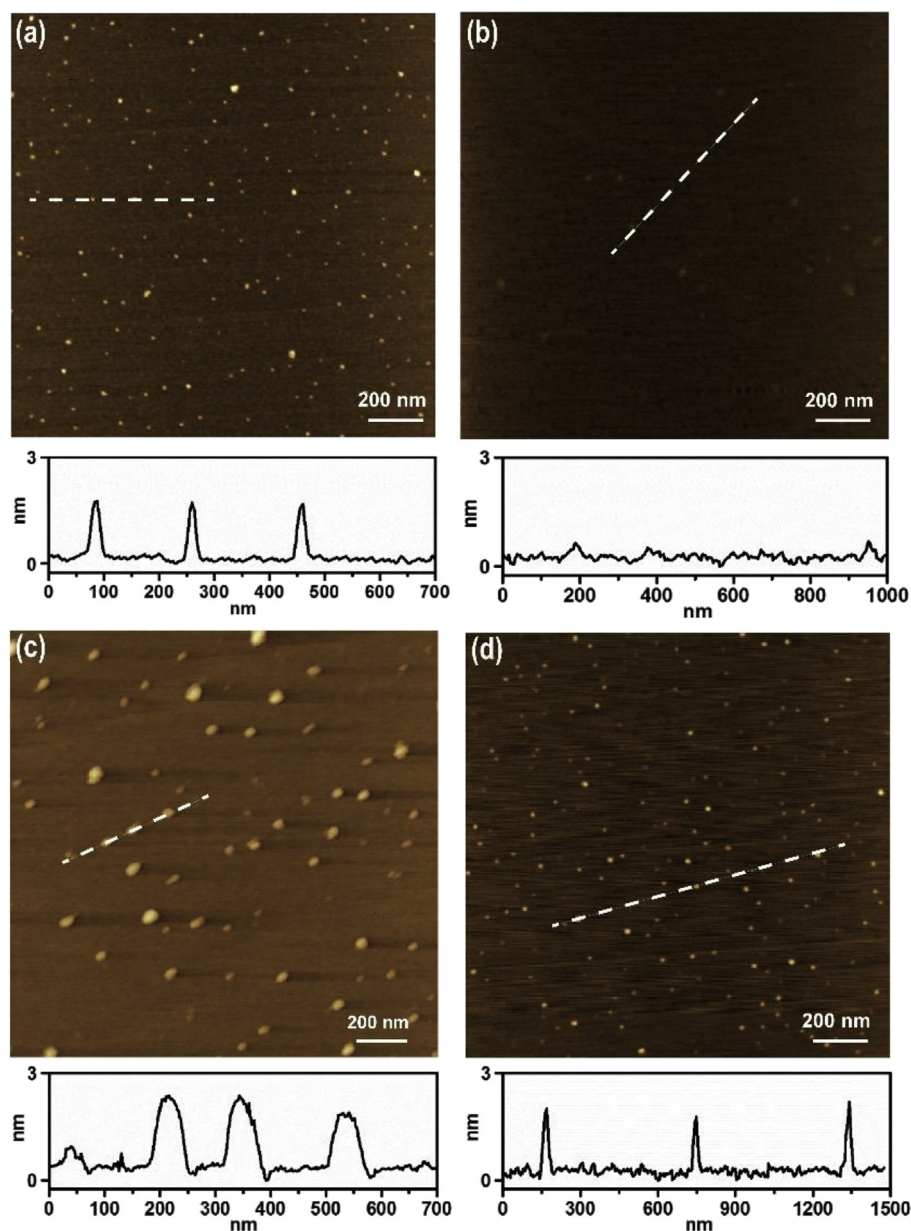


Fig. 6. Typical tapping-mode AFM height images of pure Poly-1 (a) and DiOC₂(5) (b), and the mixing with DiOC₂(5) at a [Poly-1]/[DiOC₂(5)] ratio of 1/1 (c) and 16/1 (d), respectively. Height profiles measured along the dashed lines were also shown underneath the images. The concentration of pure Poly-1 and DiOC₂(5) was 30.4 μM in water. The substrate was mica.

Poly-1 and DiOC₂(5) displayed an upward curve, indicative of both static and dynamic quenching occurring [48]. These results showed that KI quenching effect increased when DiOC₂(5) was bound to Poly-1, which was in consistent with the groove binding mode.

3.5. Mechanism of concentration-dependent DiOC₂(5) aggregation and disassembly

Obviously, the above concentration-dependent aggregation depended on the binding of DiOC₂(5) to Poly-1. To determine the driving force for the binding, we conducted isothermal titration calorimetry (ITC) measurements. Fig. 9 showed that the saturation of binding stoichiometry was at around 1:1, i.e., one monomer unit of Poly-1 per DiOC₂(5) molecule, or two monomer units per dimer. In addition, the binding constant was calculated as $1.21 \times 10^4 \text{ M}^{-1}$. Besides, the negative ΔG value of $-5.57 \times 10^3 \text{ cal mol}^{-1}$ revealed the binding of DiOC₂(5) to Poly-1 to be a spontaneous process, which was based on

electrostatic interactions between the positively charged DiOC₂(5) molecules and the negatively charged pendants of Poly-1 [49].

Usually, the cyanine dye aggregation was primarily triggered by hydrophobic and van der Waals interactions [50]. In this system, Poly-1 could act as an electrostatic three-dimensional scaffold and partly neutralized the electrostatic repulsive forces among DiOC₂(5) molecules. These positively charged molecules were located on the negatively charged Poly-1 chains, allowing the removal of water molecules from the vicinity of DiOC₂(5) aromatic groups [9]. Afterwards, the hydrophobic and van der Waals interactions played crucial roles, and thus promoted the aggregation. As a result, we found the formation of face-to-face H-dimers for DiOC₂(5). The [DiOC₂(5)]/[Poly-1] ratio of 1:1 was saturated for H-dimers to polymer chains. Moreover, H-dimers would be arranged on the top of each other based on the screw sense of templated Poly-1, resulting in the formation of chiral H-aggregates. Notably, this type of foldamer featured ~ 6 monomer units per turn [20], which could complex with three dimers. This specific

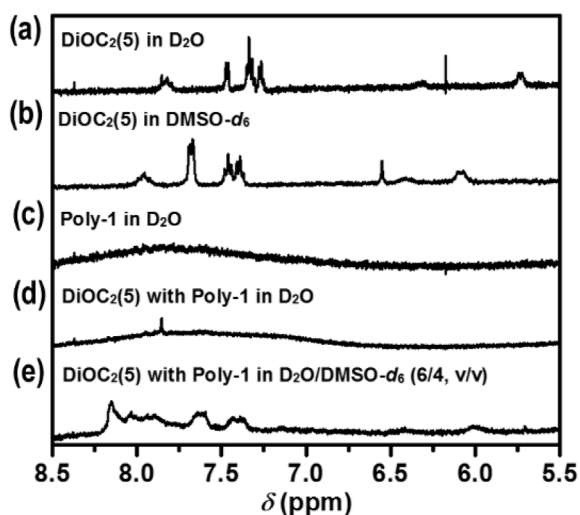


Fig. 7. ^1H NMR spectra of $\text{DiOC}_2(5)$ in D_2O (a) and $\text{DMSO-}d_6$ (b) Poly-1 in D_2O (c), and $\text{DiOC}_2(5)$ with Poly-1 in D_2O (d) and $\text{D}_2\text{O}/\text{DMSO-}d_6$ (6/4, v/v) (e) at ambient temperature. $[\text{Poly-1}] = 3.8 \text{ mM}$; $[\text{DiOC}_2(5)] = 0.24 \text{ mM}$.

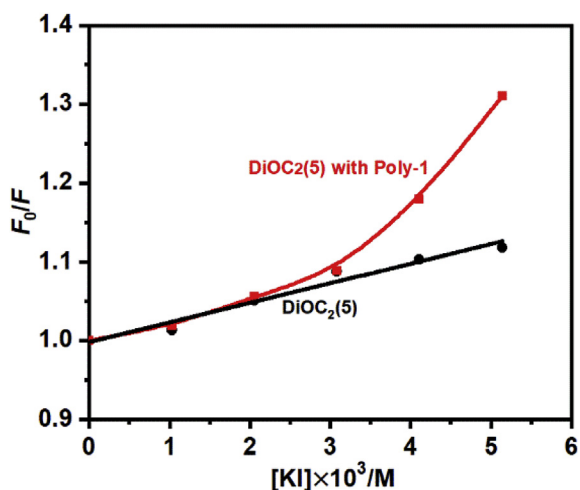


Fig. 8. Quenching of $\text{DiOC}_2(5)$ fluorescence by KI in the presence and absence of Poly-1 in water at ambient temperature. $[\text{DiOC}_2(5)] = 52 \mu\text{M}$; $[\text{Poly-1}]/[\text{DiOC}_2(5)] = 16$.

complexation was illustrated in Scheme 1b. Interestingly, despite the formation of chiral H-aggregates, the aggregates were disassembled by further addition of Poly-1 . The increase of negative charges from newly added Poly-1 led to more anion binding sites, which attracted $\text{DiOC}_2(5)$ molecules in H-aggregates. As a result, it gave rise to the disassembly of H-aggregates. In particular, these disassembled dyes were inserted into the helical grooves of Poly-1 , probably due to the hydrophobic effect, which decreased the local polarity around $\text{DiOC}_2(5)$. Consequently, the energy gap between HOMO and LUMO of the dye reduced, leading to a 22 nm red-shifted absorption band similar to the original one [51]. The H-aggregates could be completely disassembled to the monomeric molecules. More importantly, these monomers were still dispersed within the helical grooves of Poly-1 and exhibited a specific chirality, as illustrated in Scheme 1b.

4. Conclusion

In conclusion, we have demonstrated the concentration-dependent aggregation and disassembly of $\text{DiOC}_2(5)$ using a poly(phenylene-diethynylene)-based helical foldamer bearing L-alanine sodium pendants with an amide linker. When the ratio of $[\text{Poly-1}]/[\text{DiOC}_2(5)]$ was

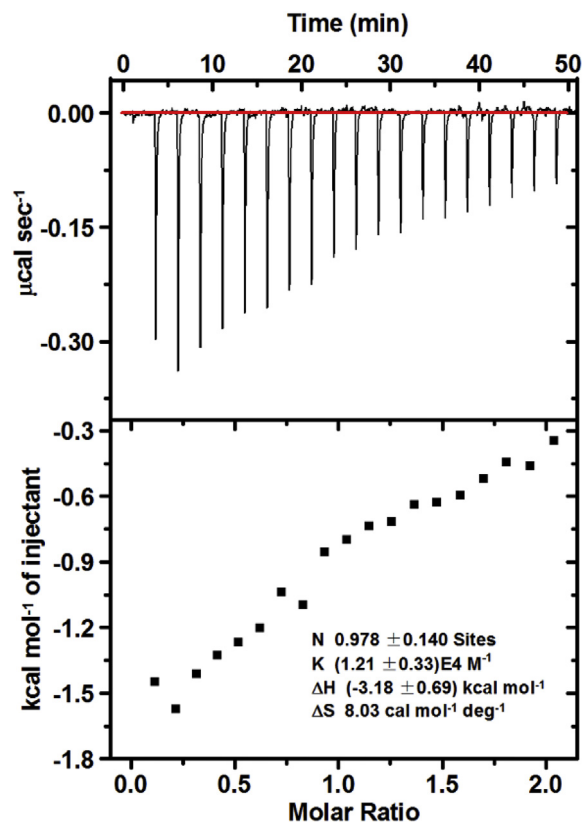


Fig. 9. Plots of heat rate versus time (up) and heat versus molar ratio of Poly-1 to $\text{DiOC}_2(5)$ (bottom) obtained from ITC experiments at 25°C .

small, chiral $\text{DiOC}_2(5)$ H-aggregates were enriched on Poly-1 surface. In contrast, when the ratio was large, $\text{DiOC}_2(5)$ molecules were inserted into the helical groove of Poly-1 in a single-molecule form. Meanwhile, the solution color underwent an obvious change. The present investigation is crucial not only in further insighting the aggregation and disassembly of cyanine dye but in widening applications ranging from sensors to high anti-counterfeits.

Acknowledgments

We acknowledge the financial support of the National Natural Science Foundation of China (51433002 and 51773070) and Research on geological technology and application of Hubei province (KJ2018-21). We also thank the HUST Analytical and Testing Center for CD and AFM Measurements.

Appendix A. Supplementary data

Supplementary data to this article can be found online at <https://doi.org/10.1016/j.polymer.2019.02.063>.

References

- [1] K.C. Hannah, B.A. Armitage, DNA-templated assembly of helical cyanine dye aggregates: a supramolecular chain polymerization, *Acc. Chem. Res.* 37 (2004) 845–853.
- [2] P.J. Clapp, B.A. Armitage, B. David F. O, Two-dimensional polymerization of lipid bilayers: visible-light-sensitized photoinitiation, *Macromolecules* 30 (1997) 32–41.
- [3] W. Sun, S. Guo, C. Hu, J. Fan, X. Peng, Recent development of chemosensors based on cyanine platforms, *Chem. Rev.* 116 (2016) 7768–7817.
- [4] P. Innocenzia, B. Lebeau, Organic-inorganic hybrid materials for non-linear optics, *J. Mater. Chem.* 15 (2005) 3821–3831.
- [5] L. Wang, J. Xiang, H. Sun, Q. Yang, L. Yu, Q. Li, A. Guan, Y. Tang, Controllable cy3-MTC-dye aggregates and its applications served as a chemosensor, *Dyes Pigments* 122 (2015) 382–388.
- [6] N. Kato, J. Prime, K. Katagiri, F. Caruso, Preparation of J-aggregate liposome

- dispersions and their chromic transformation, *Langmuir* 20 (2004) 5718–5723.
- [7] F. Nicoli, M.K. Roos, E.A. Hemmig, M.D. Antonio, R.d. Vivie-Riedle, T. Liedl, Proximity-induced H-aggregation of cyanine dyes on DNA-duplexes, *J. Phys. Chem. A* 120 (2016) 9941–9947.
- [8] Y. Zhang, J. Xiang, Y. Tang, G. Xu, W. Yan, Chiral transformation of achiral J-aggregates of a cyanine dye templated by human serum albumin, *ChemPhysChem* 8 (2007) 224–226.
- [9] S. Gadde, E.K. Batchelor, A.E. Kaifer, Controlling the formation of cyanine dye H- and J-aggregates with cucurbituril hosts in the presence of anionic polyelectrolytes, *Chem. Eur. J.* 15 (2009) 6025–6031.
- [10] C. Tan, E. Atas, J.G. Muller, M.R. Pinto, V.D. Kleiman, K.S. Schanze, Amplified quenching of a conjugated polyelectrolyte by cyanine dyes, *J. Am. Chem. Soc.* 126 (2004) 13685–13694.
- [11] F.C. Spano, The spectral signatures of Frenkel polarons in H- and J-aggregates, *Acc. Chem. Res.* 43 (2010) 429–439.
- [12] O.-K. Kim, J. Je, G. Jernigan, L. Buckley, D. Whitten, Super-helix formation induced by cyanine J-aggregates onto random-coil carboxymethyl amylose as template, *J. Am. Chem. Soc.* 128 (2006) 510–516.
- [13] S. Gadde, E.K. Batchelor, J.P. Weiss, Y. Ling, A.E. Kaifer, Control of H- and J-aggregate formation via host-guest complexation using cucurbituril hosts, *J. Am. Chem. Soc.* 130 (2008) 17114–17119.
- [14] H. Noguchi, M. Takafuji, V. Maurizot, I. Huc, H. Ihara, Chiral separation by a terminal chirality triggered P-helical quinoline oligoamide foldamer, *J. Chromatogr. A* 1437 (2016) 88–94.
- [15] S. Suzuki, F. Ishiwari, K. Nakazono, T. Takata, Reversible helix-random coil transition of poly(*m*-phenylenediethynylene) by a rotaxane switch, *Chem. Commun.* 48 (2012) 6478–6480.
- [16] Y.-Q. Huang, Q.-L. Fan, X.-F. Liu, N.-N. Fu, W. Huang, Solvent- and pH-induced self-assembly of cationic meta-linked poly(phenylene ethynylene): effects of helix formation on amplified fluorescence quenching and Förster resonance energy transfer, *Langmuir* 26 (2010) 19120–19128.
- [17] G. Lautrette, B. Wicher, B. Kauffmann, Y. Ferrand, I. Huc, Iterative evolution of an abiotic foldamer sequence for the recognition of guest molecules with atomic precision, *J. Am. Chem. Soc.* 138 (2016) 10314–10322.
- [18] Z. Liu, W. Xue, Z. Cai, G. Zhang, D. Zhang, A facile and convenient fluorescence detection of gamma-ray radiation based on the aggregation-induced emission, *J. Mater. Chem.* 21 (2011) 14487–14491.
- [19] K.K.L. Cheuk, B.S. Li, J.W.Y. Lam, Y. Xie, B.Z. Tang, Synthesis, chain helicity, assembling structure, and biological compatibility of poly(phenylacetylene)s containing L-alanine moieties, *Macromolecules* 41 (2008) 5997–6005.
- [20] K. Maeda, L. Hong, T. Nishihara, Y. Nakanishi, Y. Miyauchi, R. Kitaara, N. Ousaka, E. Yashima, H. Ito, K. Itami, Construction of covalent organic nanotubes by light-induced cross-linking of diacetylene-based helical polymers, *J. Am. Chem. Soc.* 138 (2016) 11001–11008.
- [21] C. Tan, M.R. Pinto, M.E. Kose, I. Ghiviriga, K.S. Schanze, Solvent-induced self-assembly of a meta-linked conjugated polyelectrolyte. Helix formation, guest intercalation, and amplified quenching, *Adv. Mater.* 16 (2004) 1208–1212.
- [22] H. Sogawa, M. Shiotsuki, F. Sanda, Synthesis and photoresponse of helically folded poly(phenyleneethynylene)s bearing azobenzene moieties in the main chains, *Macromolecules* 46 (2013) 4378–4387.
- [23] H. Yuan, J. Xu, E.P.V. Dam, G. Giubertoni, Y.L.A. Rezus, R. Hammink, H.J. Bakker, Y. Zhan, A.E. Rowan, C. Xing, P.H.J. Kowser, Strategies to increase the thermal stability of truly biomimetic hydrogels: combining hydrophobicity and directed hydrogen bonding, *Macromolecules* 50 (2017) 9058–9065.
- [24] J.C. Nelson, J.G. Saven, J.S. Moore, P.G. Wolynes, Solvophobically driven folding of nonbiological oligomers, *Science* 277 (1997) 1793–1796.
- [25] R.B. Prince, J.G. Saven, P.G. Wolynes, J.S. Moore, Cooperative conformational transitions in phenylene ethynylene oligomers: chain-length dependence, *J. Am. Chem. Soc.* 121 (1999) 3114–3121.
- [26] S. Suzuki, K. Matsuura, K. Nakazono, T. Takata, Effect of a side chain rotaxane structure on the helix-folding of poly(*m*-phenylene diethynylene), *Polym. J.* 46 (2014) 355–365.
- [27] M. Fujiki, Optically active polysilylenes: state-of-the-art chiroptical polymers, *Macromol. Rapid Commun.* 22 (2001) 539–563.
- [28] D.G. Peiffer, R.D. Lundberg, Synthesis and viscometric properties of low charge density ampholytic ionomers, *Polymer* 26 (1985) 1058–1068.
- [29] A. Sidorowicz, A. Pola, P. Dobryszczycki, Spectral properties of 3,3'-diethyloxadiazocyanine included in phospholipid liposomes, *J. Photochem. Photobiol., B* 38 (1997) 94–97.
- [30] T. Miyagawa, M. Yamamoto, R. Muraki, H. Onouchi, E. Yashima, Supramolecular helical assembly of an achiral cyanine dye in an induced helical amphiphilic poly(phenylacetylene) interior in water, *J. Am. Chem. Soc.* 129 (2007) 3676–3682.
- [31] W. West, S. Pearce, The dimeric state of cyanine dyes, *J. Phys. Chem.* 69 (1965) 1894–1903.
- [32] M. Wang, G.L. Silva, B.A. Armitage, DNA-templated formation of a helical cyanine dye J-aggregate, *J. Am. Chem. Soc.* 122 (2000) 9977–9986.
- [33] G. Pesciell, L.D. Bari, N. Berova, Application of electronic circular dichroism in the study of supramolecular systems, *Chem. Soc. Rev.* 43 (2014) 5211–5233.
- [34] Y. Xu, Z. Li, A. Malkovskiy, S. Sun, Y. Pang, Aggregation control of squaraines and their use as near-infrared fluorescent sensors for protein, *J. Phys. Chem. B* 114 (2010) 8574–8580.
- [35] W.Z. Yuan, P. Lu, S. Chen, J.W.Y. Lam, Z. Wang, Y. Liu, H.S. Kwok, Y. Ma, B.Z. Tang, Changing the behavior of chromophores from aggregation-caused quenching to aggregation-induced emission: development of highly efficient light emitters in the solid state, *Adv. Mater.* 22 (2010) 2159–2163.
- [36] M. Rubinstein, R.H. Colby, *Polymer Physics*, Oxford University Press, Oxford, 1998.
- [37] K. Tanaka, J. Yoon, A. Takahara, T. Kajiyama, Ultrathinning-induced surface phase separation of polystyrene/poly(vinyl methyl ether) blend film, *Macromolecules* 28 (1995) 934–938.
- [38] Y. Liao, J. You, T. Shi, L. An, P.K. Dutta, Phase behavior and dewetting for polymer blend films studied by in situ AFM and XPS: from thin to ultrathin films, *Langmuir* 23 (2007) 11107–11111.
- [39] D.G.H. Ballard, G.D. Wicnall, J. Schelten, Measurement of molecular dimensions of polystyrene chains in the bulk polymer by low angle neutron diffraction, *Eur. Polym. J.* 9 (1973) 965–969.
- [40] Y. Liao, Z. Su, Z. Sun, T. Shi, L. An, Dewetting and phase behaviors for ultrathin films of polymer blend, *Macromol. Rapid Commun.* 27 (2006) 351–355.
- [41] Y. Liao, Z. Su, X. Ye, Y. Li, J. You, T. Shi, L. An, Kinetics of surface phase separation for PMMA/SAN thin films studied by in situ atomic force microscopy, *Macromolecules* 38 (2005) 211–215.
- [42] Y. Tsujii, K. Ohno, S. Yamamoto, A. Goto, T. Fukuda, Structure and properties of high-density polymer brushes prepared by surface-initiated living radical polymerization, *Adv. Polym. Sci.* 197 (2006) 1–45.
- [43] Z. Yang, Z. Xue, Y. Liao, X. Zhou, J. Zhou, J. Zhu, X. Xie, Hierarchical hybrids of carbon nanotubes in amphiphilic poly(ethylene oxide)-block-polyaniline through a facile method: from smooth to thorny, *Langmuir* 29 (2013) 3757–3764.
- [44] S. Sakurai, K. Kuroyanagi, K. Morino, M. Kunitake, E. Yashima, Atomic force microscopy study of helical poly(phenylacetylene)s on a mica substrate, *Macromolecules* 36 (2003) 9670–9674.
- [45] P. Thordarson, Determining association constants from titration experiments in supramolecular chemistry, *Chem. Soc. Rev.* 40 (2011) 1305–1323.
- [46] S. Geng, L.S. Qing Wub, F. Cui, Spectroscopic study one thiosemicarbazone derivative with ctDNA using ethidium bromide as a fluorescence probe, *Int. J. Biol. Macromol.* 60 (2013) 288–294.
- [47] C.V. Kumart, R.S. Turner, E.H. Asuncion, Groove binding of a styrylcyanine dye to the DNA double helix: the salt effect, *J. Photochem. Photobiol. A Chem.* 74 (1993) 231–238.
- [48] T. Ikai, D. Suzuki, K. Shinohara, K. Maeda, S. Kanoh, A cellulose-based chiral fluorescent sensor for aromatic nitro compounds with central, axial and planar chirality, *Polym. Chem.* 8 (2017) 2257–2265.
- [49] C.W.T. Leung, Y. Hong, J. Hanske, E. Zhao, S. Chen, E.V. Pletneva, B.Z. Tang, Superior fluorescent probe for detection of cardiolipin, *Anal. Chem.* 86 (2014) 1263–1268.
- [50] J.O. Smith, D.A. Olson, B.A. Armitage, Molecular recognition of PNA-containing hybrids: spontaneous assembly of helical cyanine dye aggregates on PNA templates, *J. Am. Chem. Soc.* 121 (1999) 2686–2695.
- [51] D. Sarkar, P. Das, S. Basak, N. Chattopadhyay, Binding interaction of cationic phenazinium dyes with calf thymus DNA: a comparative study, *J. Phys. Chem. B* 112 (2008) 9243–9249.